MODEL-BASED PLASMA STATE CONTROL IN TOKAMAKS

D. Moreau[1,2,3], D. Mazon[1,2], Y. Adachi[3], Y. Takase[3], Y. Sakamoto[4], S. Ide[4], T. Suzuki[4] and JET-EFDA Contributors*

[1]CEA, IRFM, 13108, Saint-Paul-lez-Durance, France.
[2]JET-EFDA, Culham Science Centre, OX14 3DB, Abingdon, U.K.
[3]The University of Tokyo, Graduate School of Frontier Sciences, 277-8561, Kashiwa, Japan
[4]JAEA, Fusion Research and Development Directorate, 311-0193, Naka, Japan

Abstract

The basic elements of an integrated model-based control strategy for extrapolating present-day advanced tokamak scenarios to steady state operation are described. Taking advantage of the large ratio between the time scales involved in the magnetic and thermal diffusion processes, the model identification procedure makes use of a multiple time scale approximation. The methodology is generic and can be applied to any device, with different sets of heating and current drive actuators, controlled variables and/or parameter profiles. It has been applied to experimental data from JET and JT-60U, and satisfactory models have been obtained. A profile controller can then be articulated around two composite feedback loops operating on the resistive and confinement time scales, respectively. First experimental results obtained with three H&CD actuators to control the safety factor profile on JET are displayed. Simultaneous real-time control of the q-profile and toroidal velocity profile on JT-60U, using four groups of neutral beam injectors, has been simulated and typical results are presented.

Key words

Control of plasma. Identification. Modeling.

1. Introduction

The design of a steady state fusion reactor relies on the development of advanced tokamak operation scenarios in which a high performance magneto-thermal plasma state is achieved and controlled in real time [Gormezano *et al.*, 2007; Gribov *et al.*, 2007]. The multiple magnetic and kinetic parameter profiles that define the non-linear plasma state (safety factor, plasma density, velocity, pressure, etc …), and will need to be regulated, are known to be strongly coupled. The heating and current drive (H&CD) control actuators are generally quite constrained and their number is limited. Among the most commonly used H&CD systems are neutral beam injection (NBI), electron cyclotron resonance heating (ECRH), ion cyclotron resonance heating (ICRH) and lower hybrid current drive (LHCD). The strong linkage between the radial profiles of various plasma parameters can be seen as an advantage because the effective number of controlled variables or profiles can be reduced to a minimal set of essential ones. Once the response of the relevant parameters to variations of the actuators around a given equilibrium state has been identified, an integrated controller can be designed to regulate the global plasma state through a minimization algorithm, rather than each plasma parameter or profile accurately and separately. For any chosen set of target profiles, the closest self-consistent plasma state achievable with the available actuators will then be reached [Moreau *et al.*, 2008].

Present understanding of plasma transport phenomena is not sufficient yet to make reliable code predictions of the detailed dynamic response of the plasma profiles, in particular in the so-called advanced tokamak operation scenarios. Therefore, an identification technique [Ljung, 1999] has been developped to find an appropriate plasma response model from the analysis of experimental data. The state-space

* See the Appendix of F. Romanelli *et al.*, Proceedings of the 22nd IAEA Fusion Energy Conference 2008, Geneva, Switzerland.

model structure was derived from a simplified set of transport equations which are projected on a set of appropriate radial basis functions. The state variables appear naturally to be the variations of a magnetic variable, μ, such as the internal poloidal magnetic flux, Ψ, or inverse safety factor, ι, and some fluid/kinetic variables, ρ, such as the plasma toroidal velocity, V_{tor}, pressure, p, (or temperature, T) with respect to their reference values (their values in the reference state). After projection onto radial basis functions, a lumped-parameter version of the state space model is then derived, which reads :

$$\partial\mu/\partial t = A_{11}\,\mu(t) + A_{12}\,\rho(t) + B_{11}\,P(t) \ldots + B_{12}\,n(t) + B_{\mu V}.V_{ext}(t) \quad (1)$$

$$\varepsilon\,\partial\rho/\partial t = A_{21}\,\mu(t) + A_{22}\,\rho(t) + B_{21}\,P(t) + B_{22}\,n(t) \quad (2)$$

with inputs P(t) = [P_1(t), P_2(t), P_3(t), etc …], the heating and current drive input powers (e.g. the powers delivered by the NBI, ECRH, ICRH and LHCD systems), V_{ext}, the plasma surface loop voltage, and n(t), the plasma density. The small parameter, ε, represents the typical ratio of the thermal and resistive diffusion time scales. The model order can therefore be further reduced by using the theory of singularly perturbed systems [Kokotovitch, Khalil and O'Reilly, 1986]. It is clear from the structure of the original system that the magnetic variable, μ, has only a slow evolution. Its fast component can be set identically to zero in the two-time-scale model. We shall therefore seek two models of reduced orders, a slow model

$$\partial\mu/\partial t = A_s\mu + B_s\,u_s \;\; ; \quad \rho_s = C_s\mu + D_s\,u_s \quad (3)$$

and a fast model,

$$\partial\rho_f/\partial t = A_f\rho_f + B_f\,u_f \quad . \quad (4)$$

Here ρ_s and ρ_f are the slow and fast components, respectively, of the kinetic variables ($\rho=\rho_s+\rho_f$), and u_s and u_f are the slow and fast components, respectively, of the input vector ($u=u_s+u_f$).

In order to illustrate the model identification and control methodology, two examples will be considered in this paper. The first example refers to the control of the safety factor profile (representative of the current density profile) on JET and the second example will be dedicated to the identification, from some JT-60U experimental data, of a two-time-scale (magnetic/kinetic) state space model describing the coupled dynamics of the safety factor and toroidal rotation profiles in a non-inductive, high-bootstrap-current scenario.

2. Identification of a slow model for the control of the safety factor profile

In tokamaks, the safety factor is defined as q(x) = dΦ(x)/dΨ(x), where Φ(x) and Ψ(x) represent the toroidal and poloidal magnetic fluxes, respectively, and x is a normalized radial variable (0≤x≤1) labelling the magnetic flux surfaces. The safety factor is a non-dimensional parameter that characterizes the current density profile and the helicity of the magnetic field lines on a given toroidal flux surface. Its radial profile is important for MHD stability.

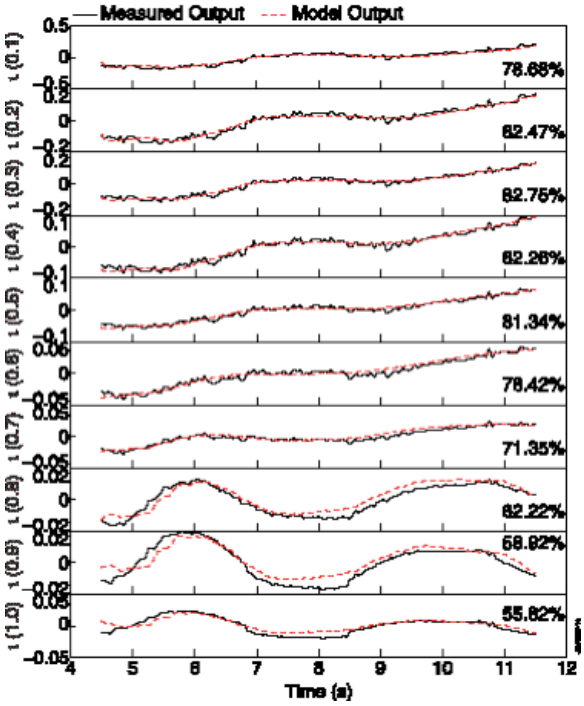

Figure 1. Coefficients of the ι(x) profile at knots x = 0.1, 0.2, 0.3, … 1. The figure shows a comparison between the experimental data and the model output. JET pulse #67840 : modulations of V_{ext} with constant H&CD powers.

In order to identify the response of the safety factor profile to variations of the control actuators around a given reference equilibrium state on JET, a number of specific open-loop experiments were performed at 3 Teslas, with a

plasma current around 1.5 MA and an average plasma density of about 3.5×10^{19} m^{-3}. The available actuators were modulated randomly around a given set of input values that define our reference state. The selected actuators consisted of : *(i)* neutral beam injection, *(ii)* ion cyclotron resonance heating, *(iii)* lower hybrid current drive, *(iv)* surface loop voltage. In order to modulate the surface loop voltage (V_{ext} in Eq. 1), the plasma boundary flux controller was requested to follow a piecewise linear boundary flux waveform. Although the safety factor, q(x), is a parameter generally used in tokamaks, it is judicious to seek a linearized model for its inverse, $\iota(x) = 1/q(x)$, because it is more linearly related to the plasma current density (through the poloidal flux) and therefore to the heating and current drive powers than q(x) itself. Thus, $\mu(x)$ stands here for $\iota(x)$ and only the slow model is needed.

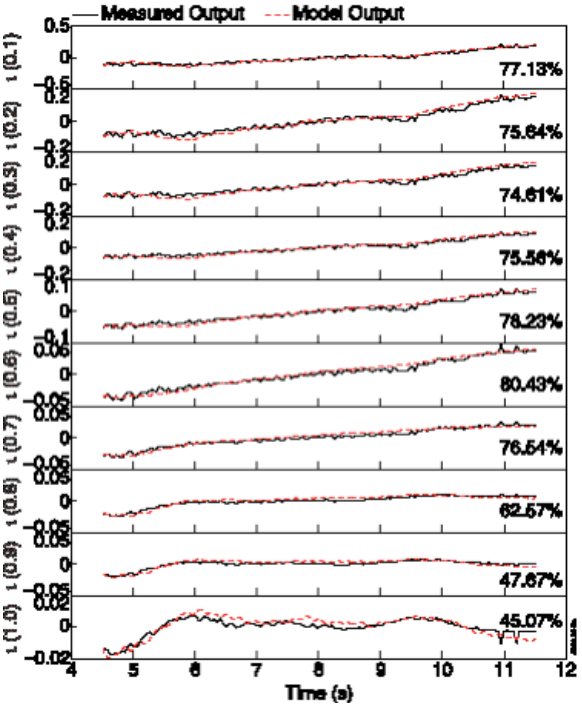

Figure 2. Coefficients of the $\iota(x)$ profile at knots x = 0.1, 0.2, 0.3, … 1. The figure shows a comparison between the experimental data and the model output. JET pulse #67874 : modulations of the NBI power with constant LH and ICRH powers, and constant request on V_{ext}.

Comparing the experimental $\iota(x)$ data with predictions using the measured inputs and the identified model shows a good agreement. Typical results are shown here, when actuators such as V_{ext} (Figure 1) or the NBI power are modulated (Figure 2).

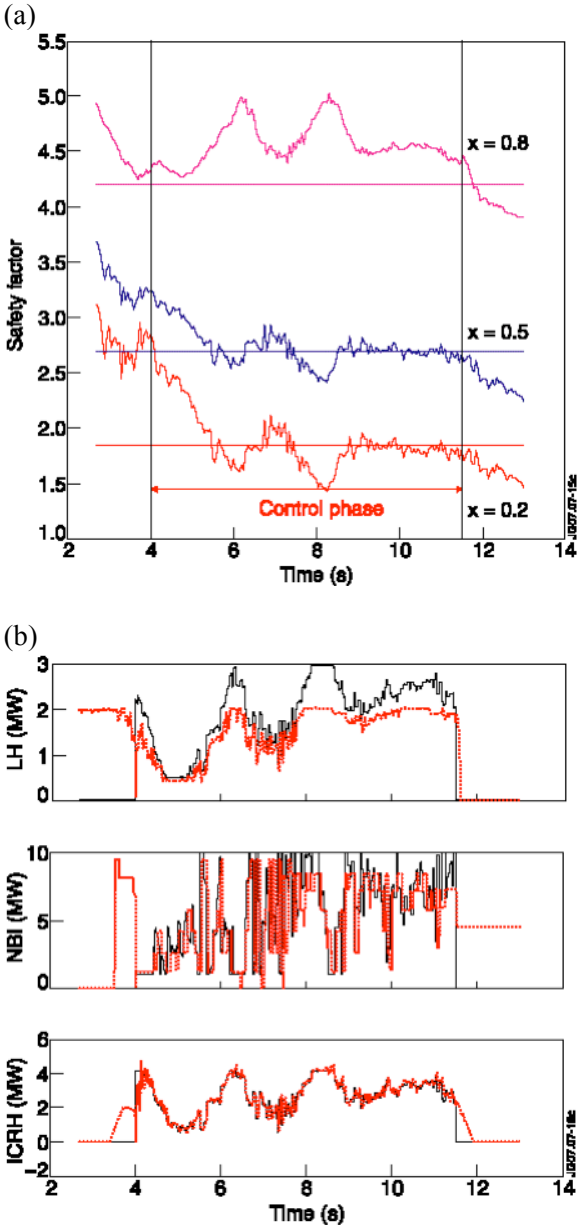

Figure 3. (a) Control of the safety factor profile at three normalized radii, x = 0.2 (red), x =0.5 (blue), and x = 0.8 (magenta) using the three H&CD actuators (Pulse #70395). During the control phase V_{ext} is requested constant (32mV/rad). Target values are represented by horizontal lines. (b) Requested (full traces) and delivered (dotted traces) LH, NBI and ICRH powers for JET pulse #70395.

Altogether, from the comparison between the experimental and the simulated data, the slow model thus identified was found to be sufficiently accurate for some closed-loop control experiments to be attempted.

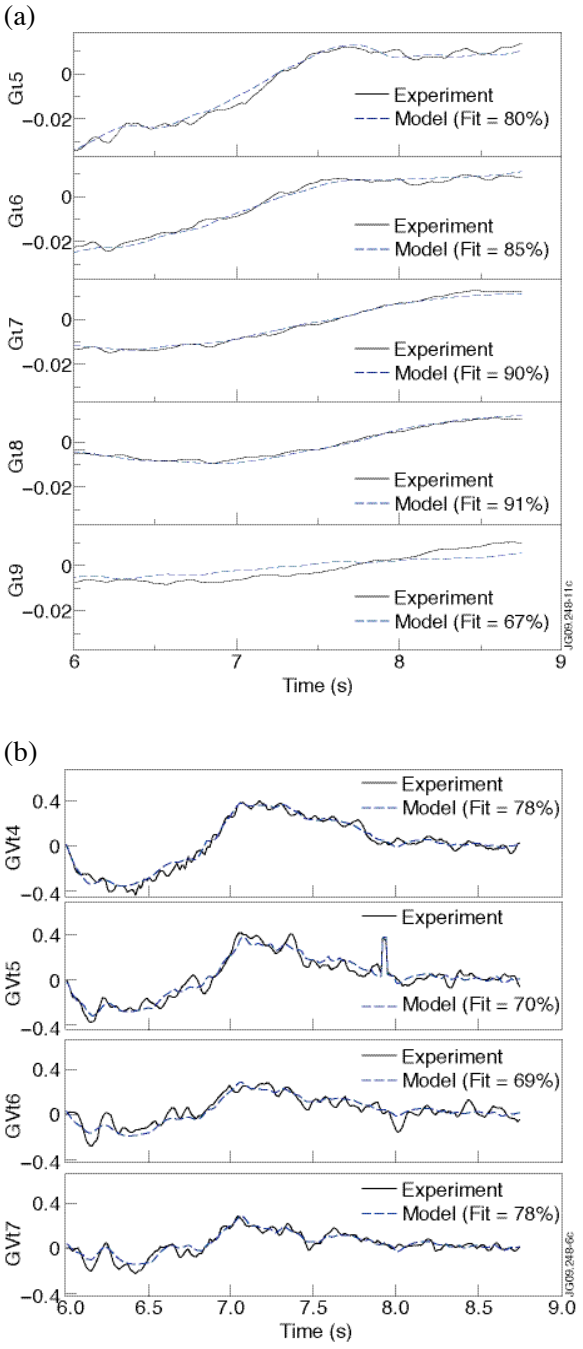

Figure 4. The figure shows a comparison between the experimental data (JT-60U pulse #45862) and the model output. (a) Slow model. Coefficients of the $\iota(x)$ profile at knots x = 0.5, 0.6, 0.7, 0.8, 0.9. (b) Fast model. Coefficients of the $V_{tor}(x)$ profile at knots x = 0.4, 0.5, 0.6, 0.7.

Figure 3 illustrates such an experiment where the controlled variables were q(x) at $x = 0.2$, 0.5 and 0.8. The corresponding target values were 1.85, 2.7 and 4.2, respectively. The controller was active between t = 4 s and t = 11.5 s, and the requested value of the surface loop voltage was 32 mV/rad during the control phase. The initial behaviour of the controller is dominated by a transient in the boundary flux control which causes large oscillations of the loop voltage and, as a consequence, of the H&CD powers. Control becomes really effective and successful when the boundary flux has finally tracked the requested waveform, and the loop voltage has settled to the desired value. Figure 3b shows a comparison between the requested actuator powers, and the delivered ones. The requested target for the q-profile was not reached exactly at $x = 0.8$ because the LH power could not exceed 2 MW while 3 MW were requested. At constant loop voltage, more LH power would have driven more current, with a larger off-axis component, decreasing q in the outer region and reducing the error around $x = 0.8$.

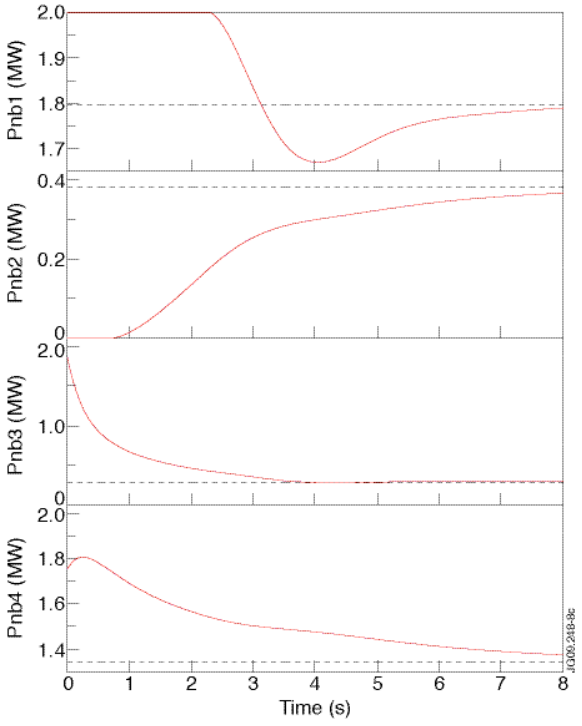

Figure 5. Evolution of the four actuator powers in a closed-loop simulation showing the simultaneous control of the safety factor and the toroidal velocity profiles on JT-60U. The time origin refers to the start of the control phase.

3. Identification of a two-time-scale model for magnetic and kinetic control

The same methodology has been applied to JT-60U data to identify a two-time-scale model for the simultaneous control of magnetic and kinetic profiles. A series of high-bootstrap-current advanced tokamak discharges were analysed. The reference plasma state was

characterized by a magnetic field of 3.7 T, a plasma current of 0.9 MA at zero loop voltage (i.e. fully non-inductively driven), and a central plasma density of 3×10^{19} m^{-3}. The selected actuators consisted of four groups of neutral beam injectors corresponding to : *(i)* on-axis perpendicular injection, *(ii)* off-axis perpendicular injection, *(iii)* on-axis co-current tangential injection, *(iv)* off-axis co-current tangential injection. The response to changes in the line-averaged density was also identified because it plays an important role in the model.

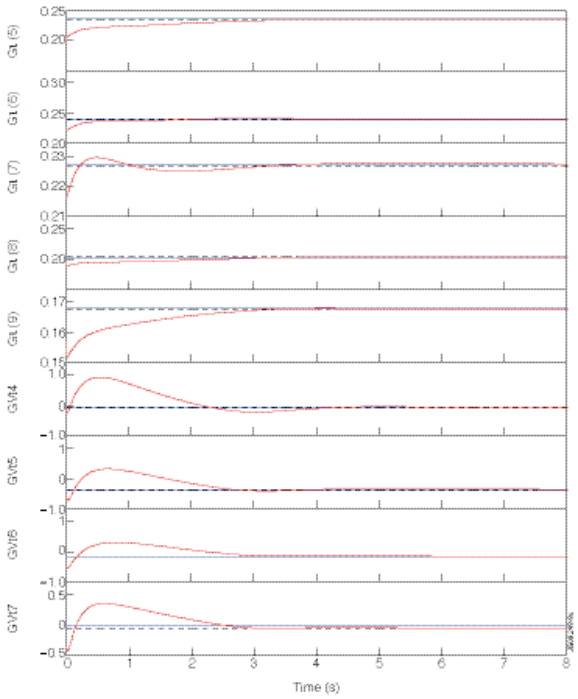

Figure 6. Evolution of $\iota(x)$ at $x = 0.5$-0.9 (5 upper traces) and $V_t(x)$ at $x = 0.4$-0.7 (4 lower traces) in the closed-loop simulation showing the simultaneous control of the safety factor and the toroidal velocity profiles on JT-60U (see also figure 4). The requested target values are represented by the horizontal lines.

The comparison between the measured data and the model simulation for the dynamics of the inverse safety factor, the toroidal plasma velocity and the ion temperature shows the good potential of the technique. An example is displayed here on Figures 4a-b. To illustrate the controller design and time response, the results of typical closed-loop simulations based on the identified two-time-scale model is also displayed on Figures 5-6. The slow and the fast reduced-order models are models of order 4 whose slowest characteristic time constants are 3.28s and 0.37s, respectively. The closed-loop simulations correspond to virtual discharges with the same field and current as the reference pulse, but with controller-driven NBI actuators. In the simulations, the inverse safety factor profile, $\iota(x)$, the toroidal velocity profile, $V_{tor}(x)$, and the ion temperature profile, $T_i(x)$, are controlled using the four groups of NBI injectors.

4. Conclusion

In conclusion, it is shown that the technique described here can be applied to different devices, for simple as well as more comprehensive controls, and with different sets of actuators and sensors. Experiments on other pulsed and steady-state tokamaks would also be beneficial to possibly validate and improve this methodology. They could provide a broad basis for developing integrated profile control and reactor relevant steady state scenarios in ITER.

Acknowledgements

This work, supported by the European Communities under the contract of Association between EURATOM and CEA, was carried out within the framework of the European Fusion Development Agreement. The views and opinions expressed herein do not necessarily reflect those of the European Commission. Part of this work was also carried out at The University of Tokyo while the first author was a visiting professor and he would like to express his gratitude to the Takase-Ejiri Laboratory for their help and hospitality.

References

Gormezano, C. *et al.* (2007) Progress in the ITER Physics Basis Chapter 6: Steady state operation, Nucl. Fusion **47** S285.

Gribov, Y. *et al.* (2007) Progress in the ITER Physics Basis Chapter 8: Plasma operation and control, Nucl. Fusion **47** S385.

Kokotovitch, P.V., Khalil, H.K. and O'Reilly, J. (1986) *Singular Perturbation Methods in Control: Analysis and Design*, Academic Press, London.

Ljung, L. (1999) *System Identification: Theory for the User*, Prenctice Hall PTR, Upper Saddle River, NJ 07458.

Moreau, D. *et al* (2008) Nucl. Fusion **48** 106001.